

Relating Follicly-Challenged Compact Stars to Bald Black Holes

Kent Yagi and Nicolás Yunes

Department of Physics, Montana State University, Bozeman, MT 59717, USA.

(Dated: April 29, 2022)

Compact stars satisfy certain no-hair relations through which their multipole moments are given by their mass, spin and quadrupole moment. These relations are approximately independent of their equation of state, relating pressure to density. Such relations are similar to the black hole no-hair theorems, but these possess event horizons inside which information that led to their formation can hide. Compact stars do not possess horizons, so whether their no-hair relations are related to the black hole ones is unclear. We here show numerically that the compact star no-hair relations approach the black hole ones as the compactness approaches that of a black hole. We moreover show that compact stars become progressively oblate in this limit, even if prolate at low compactness due to strong anisotropies.

PACS numbers: 04.30.Db,04.50Kd,04.25.Nx,97.60.Jd

The Hair Style of Black Holes. Astrophysical black holes are said to have *no hair* because their exterior gravitational field can be completely described by only two *observable* quantities: their mass and their spin angular momentum. All other information or *hair* that may have led to the formation of the black hole is hidden inside its event horizon. Electric charge is a third observable that, in principle, is also needed to fully specify the gravitational field of a black hole. Astrophysically realistic ones, however, are expected to be approximately neutral, and thus charge is typically not needed.

The baldness of black holes and General Relativity's equivalence principle [1] imply that the acceleration, and thus, the motion of small, *test* bodies around a black hole depends only on its mass and spin. This is of critical importance in astrophysics because it allows for the modeling of complicated systems without having to worry about the details of the central object. For example, the motion of stars around the black hole at the center of the Milky Way [5, 6] can be modeled gravitationally with only knowledge of the central object's mass and spin.

One way to mathematically formalize the black hole no-hair relations is by inter-relating the *multipole moments* of their exterior gravitational field. Multipole expansions are commonly employed in electrodynamics and in gravitational physics to represent fields outside and far from a localized source. For example, we can approximate the gravitational potential of a bounded source distribution as a series expansion in inverse powers of the distance, r , from the field point to the source. The coefficients in this expansion will be a product of spherical harmonics $Y_{\ell m}(\theta, \phi)$ and certain angle-independent coefficients that depend only on the properties of the source. The coefficient M_ℓ that multiplies $(1/r)^{1+\ell} Y_{\ell m}(\theta, \phi)$ is called the *mass ℓ th-pole moment*, e.g. M_0 is the mass monopole, M_2 is the mass quadrupole, etc. In addition to mass moments, General Relativity requires that one introduce *current multipole moments* S_ℓ to fully describe the gravitational field, as in electrodynamics when performing a multipolar decomposition of the vector potential. In gravity, this stems from the need to decompose

the field generated by *gravitational currents*, induced either by the motion of bodies or their spin [7].

The no-hair theorems for black holes then imply that, in the multipole expansion of their exterior gravitational field, only 2 multipole moments are independent and all others can be expressed in terms of these two. The independent ones for black holes are the mass, M , which corresponds to the mass monopole moment M_0 , and the spin angular momentum, $S \equiv |\vec{S}|$, which corresponds to the current dipole moment S_1 . All other multipole moments (of order $\ell \geq 2$) are given by [8, 9]

$$M_\ell^{\text{BH}} + iS_\ell^{\text{BH}} = M \left(i \frac{S}{M} \right)^\ell. \quad (1)$$

Thus, for example, we have that $(M_0^{\text{BH}}, S_0^{\text{BH}}) = (M, 0)$, $(M_1^{\text{BH}}, S_1^{\text{BH}}) = (0, S)$, $(M_2^{\text{BH}}, S_2^{\text{BH}}) = (-S^2/M, 0)$, $(M_3^{\text{BH}}, S_3^{\text{BH}}) = (0, -S^3/M^2)$, etc.

These astonishing results were proven analytically in the late '60s and '70s by Robinson [10], Israel [11, 12], Hawking [13, 14], and Carter [8]. Their work relied on a few assumptions, such as that black holes are vacuum solutions to the Einstein equations with non-degenerate event horizons and that spacetime is real and analytic. Non-vacuum solutions to these equations, such as those that represent stars, evade the no-hair theorems, and thus, the multipole expansion of the exterior gravitational field of stars should depend on an infinite number of *independent* multipole moments. This implies that a large number of multipole moments must be independently measured before the trajectory of test bodies around stars can be predicted to high accuracy.

This is very much the case for the motion of satellites in the exterior gravitational field of Earth. The multipole expansion of the latter depends on an infinite number of independent multipole moments that encode information about Earth's interior structure and its shape. In practice, of course, only a finite number of multipole moments are needed to predict the motion of satellites in orbit around Earth with finite accuracy. The NASA mission GRACE has measured the first 360 multipole moments

of Earth [15], which allows the modeling of satellite trajectories with errors of $\mathcal{O}(R_E/r)^{361}$, with r the distance from the satellite to Earth and R_E Earth's radius.

The Hair Style of Compact Stars. The non-applicability of the no-hair theorem extends, in principle, to all stars, including compact ones, such as neutron stars and strange quark stars. There is therefore no reason to expect stars to be bald, i.e. for their exterior gravitational field to be independent of their internal structure. Moreover, different types of stars have different internal compositions, i.e. different *equations of state* relating internal pressure and density. Thus, one expects the hair of neutron stars to be different from that of white dwarfs and main sequence stars.

Recently, however, compact stars with isotropic pressure were shown to satisfy certain *approximate* no-hair relations [16–20]. That is, all multipole moments in the multipole expansion of the exterior gravitational field of compact stars can be expressed in terms of only three observable quantities. The first two are the mass (mass monopole) and spin (current dipole) of the compact star, while the third is the star's mass quadrupole moment. The independent measurement of these three observables allows us to determine all others through [19, 20]

$$M_\ell + i \left(\frac{qM}{S} \right) S_\ell = B_{\lfloor \frac{\ell-1}{2} \rfloor} M (iq)^\ell, \quad (2)$$

for $\ell > 2$ and where $\lfloor x \rfloor$ stands for the largest integer not exceeding x , the parameter q is related to the mass quadrupole moment M_2 via $q = -i(M_2/M)^{1/2}$, and B_ℓ is a pure number that in principle depends on the compact stars's equation of state. For example, Eq. (2) implies that $S_3 = B_1 S q^2$, $M_4 = B_1 M q^4$, etc. Although these relations were originally derived in a low compactness expansion, i.e. assuming that the ratio of the compact star mass to its radius is small, they were recently extended and confirmed numerically for compact stars with realistic and high compactnesses [20].

These inter-relations between multipole moments correspond to compact star no-hair relations *if and only if* they are independent of the compact star's internal structure, or more specifically, independent of its equation of state. Equation (2) depends on the equation of state only through the coefficients B_ℓ . These coefficients have been shown to take on *approximately the same numerical value* (up to percent differences) within a very large class of compact star equations of state [19, 20], including tabulated ones constructed from approximate solutions to certain many-body quantum equations [21–27]. Such equation-of-state independence has been verified in a variety of scenarios, including larger families of equations of state [28, 29], using expansions in powers of the stellar compactness [19, 29, 30], including magnetic fields [31], and allowing for arbitrary spin magnitudes [18, 20, 32] in full General Relativity [20]. Thus, we say that compact stars are *approximately bald or follicly challenged*.

But what is the origin of these approximate no-hair relations? In the black hole case, one argues that all

details of the matter distribution that formed the black hole are hidden behind its event horizon. This explanation fails for compact stars since they do not possess an event horizon. Thus, in principle, details of their interior matter distribution need not be hidden from the outside and could affect their exterior gravitational field. Recently, Ref. [33] proposed a phenomenological picture to explain the approximate no-hair relations: as some set of parameters (such as the compactness or temperature of the star) are tuned beyond a given threshold, an *approximate symmetry emerges* that is not present in general. In particular, they found that as compactness is increased, radial profiles of the eccentricity (a measure of the degree of ellipticity of the star at the equator) become nearly constant throughout the star, leading to the *emergence of isodensity self-similarity*.

Are the black hole and compact star no-hair relations related? If one pushes the phenomenological picture of [33] to the extreme and “flows” toward the black hole region of phase space by increasing compactness to 1/2 (the compactness of a non-spinning, Schwarzschild black hole), one encounters a problem. Black holes have all of their mass concentrated at their singularity, and thus, there is no matter density elsewhere in their interior with which to construct self-similar isodensity contours. It is thus not obvious or clear that the approximate no-hair relations will approach the black hole ones *continuously* as an unstable compact star collapses into a black hole.

This topic was recently tackled in [34] by considering neutron stars with anisotropic pressure, since the latter allows for stars with compactnesses close to those of black holes. Reference [34] calculated the tidal deformations of such an anisotropic star due to a secondary body to leading-order in an expansion in powers of compactness. Their results indicated that strongly-anisotropic, incompressible stars become *prolate* when perturbed (i.e. ellipsoids with the semi-major axis aligned with the axis of rotation). If this remained true in the high-compactness regime, it would be in stark contrast to perturbed black holes, which have been long shown to be *oblate* when deformed [35]. The shape of a star is controlled, among other things, by its quadrupole moment, and thus, if a neutron star with compactnesses close to that of a black hole is prolate instead of oblate, its quadrupole moments must not be approaching that of a black hole. The work of [34] then suggests that the approximate no-hair relations for compact stars may not approach the black hole ones as the compactness increases.

Let us revisit anisotropic neutron stars and quark stars with high compactness but this time in full General Relativity, instead of in a leading-order expansion in compactness. We concentrate on slowly-rotating stars, following the Hartle-Thorne approach [36, 37]. Slowly-rotating, anisotropic neutron star solutions have been constructed in [38, 39] to linear order in spin, i.e. in the ratio of the spin angular momentum to its mass squared, and we here extend such a calculation to third order for the first time. We also assume the stars are neutral, so that electro-

magnetic fields can be neglected. These are suitable approximations for old compact stars. We model matter anisotropy through the stress-energy tensor [39, 40]

$$T_{\mu\nu} = \rho u_\mu u_\nu + p k_\mu k_\nu + q \Pi_{\mu\nu}, \quad (3)$$

where ρ is the matter density, p is the radial pressure (assumed to be barotropic $p = p(\rho)$), q is the tangential pressure (responsible for anisotropy), u^μ is the fluid's four-velocity, k^μ is a radial vector, and $\Pi_{\mu\nu} = g_{\mu\nu} + u_\mu u_\nu - k_\mu k_\nu$ is a projection operator onto a two-dimensional surface orthogonal to u^μ and k^μ . The unit radial vector is spacelike ($g^{\mu\nu} k_\mu k_\nu = 1$), while the four-velocity is timelike ($g^{\mu\nu} u_\mu u_\nu = -1$) and parameterized through $u^\mu = u^0(1, 0, 0, \Omega)$, where u^0 is a normalization constant and Ω is the spin angular velocity.

Matter anisotropy is encoded in the tangential pressure, which we rewrite as $q = p - \sigma$ with σ the *anisotropy parameter*. We expand the latter in the slow-rotation approximation, so that its leading-order in Ω term is only a function of radius. We parameterize this function in the Bowers and Liang (BL) [42] framework

$$\sigma_{\text{BL}} = \frac{\lambda_{\text{BL}} (\rho + 3p)(\rho + p)}{3} \frac{1}{1 - 2M(r)/r} r^2 + \Omega^2 f(h_{\mu\nu}) + \mathcal{O}(\Omega^4), \quad (4)$$

where $M(r)$ is the mass interior to radius r and $f(h_{\mu\nu})$ is a function of the metric perturbation at quadratic order in spin. Clearly, one recovers isotropic stars when $\lambda_{\text{BL}} = 0$, which forces $\sigma = 0$ and thus $q = p$, so that $T_{\mu\nu}$ is the stress-energy of a perfect fluid with isotropic pressure.

We here consider anisotropic compact stars because anisotropy allows us to explore the properties of stars with compactnesses close to those of black holes. In the BL model, incompressible stars reach the black hole limit when $\lambda_{\text{BL}} = -2\pi$. Reference [34] used this model in a leading-order expansion in compactness and found that the quadrupole moment changes sign at $\lambda_{\text{BL}} = -0.8\pi$. Astrophysically, however, old compact stars are expected to be close to isotropic, with small anisotropy perhaps induced by stellar solid cores [43], magnetic fields [44], phase transitions [45, 46], or two-fluid models (normal and superfluid components) that are mathematically well-approximated by a single anisotropic fluid [47].

With these models for matter anisotropy, we can now construct anisotropic compact star solutions in General Relativity. We first expand the Einstein field equations in the slow-rotation approximation, as done by Hartle and Thorne [36, 37]. We then specify a particular equation of state for the radial pressure, such as a tabulated one [21–27] or a polytropic one of the form $p = K\rho^n$, where K and n are the polytropic constant and index respectively. With this, we can now solve the expanded equations numerically and order by order in Ω , adapting our numerical code developed in [16, 17, 20]. Note that because we work in the slow-rotation approximation and we solve the expanded equations order by order in Ω , we do not need to specify a given value of the angular velocity [36, 37]. The numerical solution can then be used

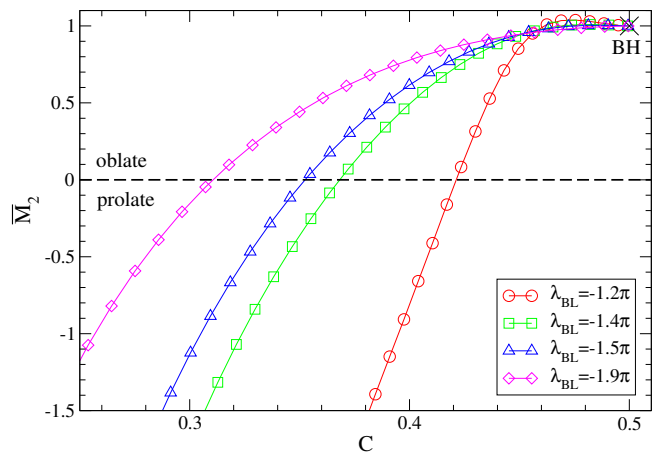


FIG. 1. (Color online) Compactness dependence of \bar{M}_2 for strongly anisotropic compact stars with an $n = 0$ polytropic equation of state. The black hole value of \bar{M}_2 is shown with a cross on the top right corner.

to extract the multipole moments of the compact star's exterior gravitational field far from the star [48, 49], as explained e.g. in [50].

Change in the stellar shape and critical behavior. Figure 1 shows the quadrupole moment normalized to its black hole value, $\bar{M}_2 \equiv M_2/M_2^{\text{BH}}$, as a function of stellar compactness, $C = M_*/R_*$, where M_* and R_* are the mass and radius of the compact star in the non-spinning configuration. Every point in this figure corresponds to the numerical construction of a compact star, with different compactness obtained by increasing the central density. Observe that $\bar{M}_2 < 0$ in the low compactness region, and thus the star is prolate as predicted by [34]. As compactness is increased, however, \bar{M}_2 becomes positive and the star becomes oblate. These results imply that relativistic corrections (proportional to high powers of compactness) change the results of [34], forcing stars to become oblate and approach the black hole expectation.

Figure 1 also shows that as the stellar compactness approaches C_{BH} , the mass quadrupole approaches the black hole result, irrespective of the value of λ_{BL} . This result *suggests* that we physically interpret the transition from a compact star to a black hole as a *continuous phase transition*, where the order parameter is the density (finite in the compact star phase and zero in the black hole phase) and the temperature (the free parameter along which the transition occurs) is the compactness, with critical value C_{BH} . Defining $\tau \equiv (C_{\text{BH}} - C)/C_{\text{BH}}$, we can then investigate the critical exponent of the multipole moments near this phase transition by computing $k_{\bar{A}_\ell} = \lim_{\tau \rightarrow 0} \ln[\bar{A}_\ell(\tau) - 1]/\ln(\tau)$, where \bar{A}_ℓ is any of the mass multipoles M_ℓ or current multipoles S_ℓ , normalized to their black hole values. For example, $\bar{S}_1 = S_1/S_1^{\text{BH}}$, where $S_1^{\text{BH}} = I^{\text{BH}}\Omega = 4M^3\Omega$ [17] and I^{BH} is the moment of inertia of a non-rotating black hole, while $\bar{S}_3 = S_3/S_3^{\text{BH}}$, where $S_3^{\text{BH}} = -S^3/M^2$ by Eq. (1). Doing so, we find that $(\bar{A}_\ell - 1) \propto \tau^{k_{\bar{A}_\ell}}$ near $\tau = 0$, with $k_{\bar{A}_\ell}$ pre-

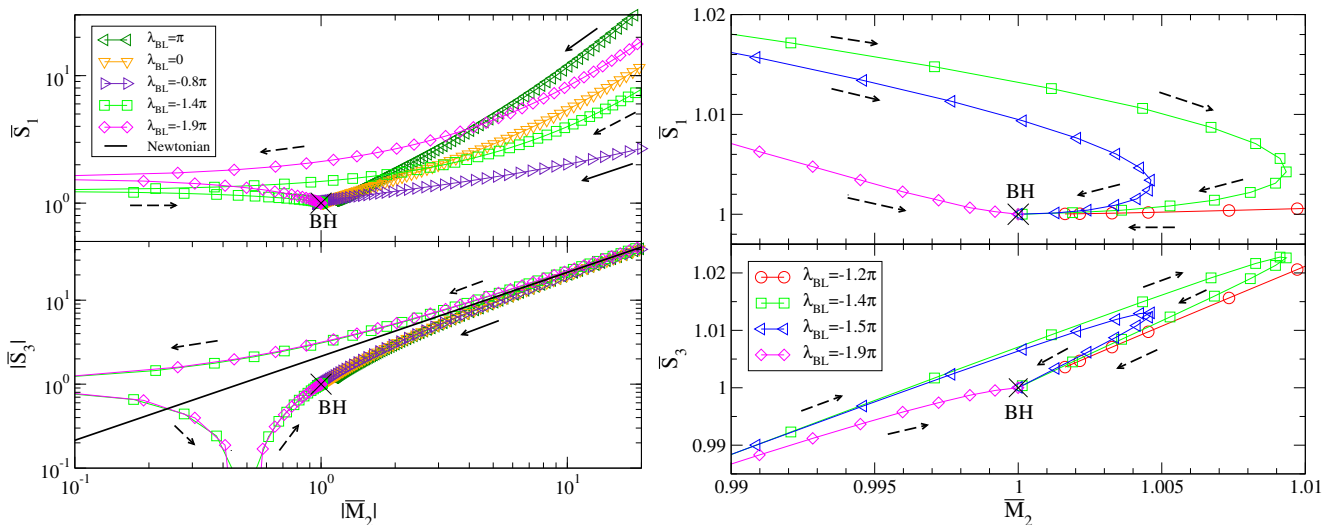


FIG. 2. (Color online) \bar{S}_1 - \bar{M}_2 (top left) and \bar{S}_3 - \bar{M}_2 (bottom left) relations for anisotropic stars model with an $n = 0$ polytropic equation of state. The right panel zooms in to the black hole limit, shown with crosses. The arrows indicate the direction of increasing compactness, with the solid ones corresponding to stars with $\lambda_{BL} \geq -0.8\pi$ and the dashed one for stars with $\lambda_{BL} < -0.8\pi$. The solid line in the bottom left panel represents the analytic Newtonian relation, which is independent of λ_{BL} .

sented in Table I. Observe that *all* multipole moments of isotropic compact stars approach the critical point at the same rate – as a fourth-order polynomial. This behavior is approximately equation-of-state universal, with variations in $k_{\bar{A}_\ell}$ of only $\sim 10\%$ due to the equation of state. Table I also shows that the mass and current multipole moments of strongly-anisotropic compact stars approach the black hole limit linearly and quadratically.

Approaching the Black Hole Limit. Let us now investigate how the approximate no-hair relations for compact stars approach the black hole no-hair relations. To see this, let us explore a sequence of compact stars of increasing compactness and plot the first few low- ℓ multipole moments, normalized to the black hole values.

Figure 2 shows this sequence for anisotropic stars with an $n = 0$ polytropic equation of state. As in Fig. 1, every point represents a different compact star constructed numerically, with different compactness obtained by in-

creasing the central density. The arrows indicate the direction of increasing compactness, and the right panel is a zoom into the black hole limit region. Observe that in the lower-compactness region (top right region of the bottom left panel) the multipole moments approach the approximate no-hair relations (shown as a black solid line labeled) expanded to lowest order in compactness, i.e. the so-called *Newtonian* approximate no-hair relations of [19] extended to anisotropic Newtonian stars. Observe also that isotropic stars tend to the black hole result, but do not reach it, since these stars do not reach sufficiently high compactnesses, e.g. the maximum compactness of a uniform density, isotropic star is 0.444 [17].

Finally, observe that anisotropic stars, which can sample compactnesses much closer to C_{BH} , continuously approach the black hole limit. Interestingly, anisotropic stars with $\lambda_{BL} \geq -0.8\pi$ approach the black hole limit directly (solid arrows), while those with $\lambda_{BL} < -0.8\pi$ (dashed arrows) overshoot it, but then turn around and approach it, while simultaneously becoming oblate. We have confirmed the behavior of \bar{S}_1 analytically by solving the Einstein equations to linear order in spin when $\lambda_{BL} = -2\pi$ in terms of hypergeometric functions. These analytic results will be presented elsewhere [51].

Future Directions. Future work could focus on showing how the approximate no-hair relations for unstable, isotropic compact stars change as they under go grav-

λ_{BL}	Isotropic	Anisotropic (poly. n=0)			
	0	-1.2π	-1.4π	-1.5π	-1.9π
$k_{\bar{S}_1}$	$3.90(\pm 0.49)$	2.20	2.08	2.03	1.87
$k_{\bar{M}_2}$	$4.22(\pm 0.45)$	1.32	1.12	1.08	1.15
$k_{\bar{S}_3}$	$4.19(\pm 0.49)$	1.30	1.10	1.06	1.93

TABLE I. Critical exponents of the multipole moments for compact stars. For isotropic stars, we present the averaged critical exponent over various equations of state, with the maximum deviations from the mean denoted in parenthesis. For anisotropic stars, we present each critical exponent as a function of the anisotropy parameter λ_{BL} , keeping the equation of state fixed to an $n = 0$ polytrope.

izational collapse and become black holes *dynamically*. Other future work could concentrate on whether this limiting behavior observed for anisotropic compact stars in General Relativity persists in other modified gravity theories. The latter will be presented elsewhere in a longer

manuscript.

Acknowledgments: We would like to thank Neil Cornish, Bennet Link, Dana Longcope and Leo Stein for useful discussions. NY acknowledges support from NSF CAREER Award PHY-1250636.

-
- [1] C. M. Will, Living Reviews in Relativity **9**, 3 (2006), arXiv:gr-qc/0510072.
- [2] D. N. Page and K. S. Thorne, Astrophys.J. **191**, 499 (1974).
- [3] K. S. Thorne, Astrophys.J. **191**, 507 (1974).
- [4] T. Johannsen, Phys.Rev. **D90**, 064002 (2014).
- [5] A. Ghez, G. Duchene, K. Matthews, S. D. Hornstein, A. Tanner, *et al.*, Astrophys.J. **586**, L127 (2003), arXiv:astro-ph/0302299 [astro-ph].
- [6] C. M. Will, (2007), arXiv:0711.1677 [astro-ph].
- [7] C. W. Misner, K. Thorne, and J. A. Wheeler, *Gravitation* (W. H. Freeman & Co., San Francisco, 1973).
- [8] B. Carter, Phys.Rev.Lett. **26**, 331 (1971).
- [9] R. O. Hansen, J. Math. Phys. **15**, 46 (1974).
- [10] D. Robinson, Phys.Rev.Lett. **34**, 905 (1975).
- [11] W. Israel, Phys. Rev. **164**, 1776 (1967).
- [12] W. Israel, Commun.Math.Phys. **8**, 245 (1968).
- [13] S. Hawking, Phys.Rev.Lett. **26**, 1344 (1971).
- [14] S. W. Hawking, Commun. Math. Phys. **25**, 152 (1972).
- [15] B. D. Tapley, S. Bettadpur, M. Watkins, and C. Reigber, Geophysical Research Letters **31**, L09607 (2004).
- [16] K. Yagi and N. Yunes, Science **341**, 365 (2013), arXiv:1302.4499 [gr-qc].
- [17] K. Yagi and N. Yunes, Phys. Rev. D **88**, 023009 (2013), arXiv:1303.1528 [gr-qc].
- [18] G. Pappas and T. A. Apostolatos, Phys.Rev.Lett. **112**, 121101 (2014), arXiv:1311.5508 [gr-qc].
- [19] L. C. Stein, K. Yagi, and N. Yunes, Astrophys.J. **788**, 15 (2014), arXiv:1312.4532 [gr-qc].
- [20] K. Yagi, K. Kyutoku, G. Pappas, N. Yunes, and T. A. Apostolatos, Phys.Rev. **D89**, 124013 (2014), arXiv:1403.6243 [gr-qc].
- [21] A. Akmal, V. Pandharipande, and D. Ravenhall, Phys.Rev. **C58**, 1804 (1998), arXiv:nucl-th/9804027 [nucl-th].
- [22] F. Douchin and P. Haensel, Astron. Astrophys. **380**, 151 (2001).
- [23] J. M. Lattimer and F. Douglas Swesty, Nuclear Physics A **535**, 331 (1991).
- [24] H. Shen, H. Toki, K. Oyamatsu, and K. Sumiyoshi, Nuclear Physics A **637**, 435 (1998).
- [25] H. Shen, H. Toki, K. Oyamatsu, and K. Sumiyoshi, Progress of Theoretical Physics **100**, 1013 (1998).
- [26] R. B. Wiringa, V. Fiks, and A. Fabrocini, Phys.Rev. **C38**, 1010 (1988).
- [27] M. Alford, M. Braby, M. Paris, and S. Reddy, Astrophys.J. **629**, 969 (2005), arXiv:nucl-th/0411016 [nucl-th].
- [28] J. M. Lattimer and Y. Lim, ApJ. 771, **51** (2013), 10.1088/0004-637X/771/1/51, arXiv:1203.4286 [nucl-th].
- [29] K. Chatziioannou, K. Yagi, and N. Yunes, Phys.Rev. **D90**, 064030 (2014), arXiv:1406.7135 [gr-qc].
- [30] T. Chan, A. P. O. Chan, and P. Leung, (2014), arXiv:1411.7141 [astro-ph.SR].
- [31] B. Haskell, R. Ciolfi, F. Pannarale, and L. Rezzolla, Mon. Not. Roy. Astron. Soc. **438**, L71 (2014), arXiv:1309.3885 [astro-ph.SR].
- [32] S. Chakrabarti, T. Delsate, N. Gurlebeck, and J. Steinhoff, Phys.Rev.Lett. **112**, 201102 (2014), arXiv:1311.6509 [gr-qc].
- [33] K. Yagi, L. C. Stein, G. Pappas, N. Yunes, and T. A. Apostolatos, Phys.Rev. **D90**, 063010 (2014), arXiv:1406.7587 [gr-qc].
- [34] K. Glampedakis, S. J. Kapadia, and D. Kennefick, Phys.Rev. **D89**, 024007 (2014), arXiv:1312.1912 [gr-qc].
- [35] E. Poisson, Phys.Rev. **D80**, 064029 (2009), arXiv:0907.0874 [gr-qc].
- [36] J. B. Hartle, Astrophys.J. **150**, 1005 (1967).
- [37] J. B. Hartle and K. S. Thorne, Astrophys. J. **153**, 807 (1968).
- [38] S. S. Bayin, Phys.Rev. **D26**, 1262 (1982).
- [39] H. O. Silva, C. F. B. Macedo, E. Berti, and L. C. B. Crispino, (2014), arXiv:1411.6286 [gr-qc].
- [40] D. D. Doneva and S. S. Yazadjiev, Phys.Rev. **D85**, 124023 (2012), arXiv:1203.3963 [gr-qc].
- [41] D. Horvat, S. Ilijic, and A. Marunovic, Class.Quant.Grav. **28**, 025009 (2011), arXiv:1010.0878 [gr-qc].
- [42] R. L. Bowers and E. P. T. Liang, Astrophys. J. **188**, 657 (1974).
- [43] R. Kippenhahn and A. Weigert, *Stellar Structure and Evolution*, XVI, 468 pp. 192 figs.. Springer-Verlag Berlin Heidelberg New York. Also *Astronomy and Astrophysics Library* (1990).
- [44] S. Yazadjiev, Phys.Rev. **D85**, 044030 (2012), arXiv:1111.3536 [gr-qc].
- [45] R. Sawyer, Phys.Rev.Lett. **29**, 382 (1972).
- [46] B. Carter and D. Langlois, Nucl.Phys. **B531**, 478 (1998), arXiv:gr-qc/9806024 [gr-qc].
- [47] P. S. Letelier, Phys. Rev. D **22**, 807 (1980).
- [48] K. S. Thorne, Rev. Mod. Phys. **52**, 299 (1980).
- [49] Y. Gürsel, Gen. Rel. Grav. **15**, 737 (1983).
- [50] G. Pappas and T. A. Apostolatos, Phys.Rev.Lett. **108**, 231104 (2012), arXiv:1201.6067 [gr-qc].
- [51] N. Yagi, K. and Yunes, in progress (2015).